

# The Processing and Impact of Dissolved Riverine Nitrogen in the Arctic Ocean

Suzanne E. Tank · Manfredi Manizza ·  
Robert Max Holmes · James W. McClelland ·  
Bruce J. Peterson

Received: 29 May 2010 / Revised: 28 April 2011 / Accepted: 19 May 2011 / Published online: 11 June 2011  
© The Author(s) 2011. This article is published with open access at Springerlink.com

**Abstract** Although the Arctic Ocean is the most riverine-influenced of all of the world's oceans, the importance of terrigenous nutrients in this environment is poorly understood. This study couples estimates of circumpolar riverine nutrient fluxes from the PARTNERS (Pan-Arctic River Transport of Nutrients, Organic Matter, and Suspended Sediments) Project with a regionally configured version of the MIT general circulation model to develop estimates of the distribution and availability of dissolved riverine N in the Arctic Ocean, assess its importance for primary production, and compare these estimates to potential bacterial production fueled by riverine C. Because riverine dissolved organic nitrogen is remineralized slowly, riverine N is available for uptake well into the open ocean. Despite this, we estimate that even when recycling is considered, riverine N may support

0.5–1.5 Tmol C year<sup>-1</sup> of primary production, a small proportion of total Arctic Ocean photosynthesis. Rapid uptake of dissolved inorganic nitrogen coupled with relatively high rates of dissolved organic nitrogen regeneration in N-limited nearshore regions, however, leads to potential localized rates of riverine-supported photosynthesis that represent a substantial proportion of nearshore production.

**Keywords** Arctic Ocean · Primary Production · Land–ocean coupling · Estuarine processes · Riverine nutrients · Dissolved organic matter · Photodegradation

## Introduction

The Arctic Ocean is the most riverine-influenced of all the world's oceans, with freshwater inputs great enough to create an estuarine-like environment throughout the ocean basin that is characterized by low-salinity surface waters with a clear terrigenous chemical signal (Opsahl et al. 1999; McClelland et al. 2011b). Freshwater discharge to the Arctic Ocean is increasing around much of the Pan-Arctic domain, with major increases from Eurasian rivers beginning in the 1960s (Peterson et al. 2002; McClelland et al. 2006) and considerable increases from North American rivers beginning in 1989, after several decades of declines (Déry and Wood 2005; Déry et al. 2009). Déry et al. (2009) also note that yearly discharge variability is increasing. These increases in discharge, coupled with changes occurring on land, are expected to lead to changing fluxes of water-borne nutrients and organic matter from land to the ocean (e.g., Striegl et al. 2005; Raymond et al. 2007; Walvoord and Striegl 2007). Understanding the current role of riverine nutrients in the Arctic Ocean is critical to our ability to detect future change.

---

S. E. Tank (✉) · B. J. Peterson  
The Ecosystems Center, Marine Biological Laboratory,  
Woods Hole, MA, USA  
e-mail: setank@mbl.edu

M. Manizza  
Department of Earth, Atmospheric, and Planetary Sciences,  
Massachusetts Institute of Technology,  
Cambridge, MA, USA

R. M. Holmes  
Woods Hole Research Center,  
Falmouth, MA, USA

J. W. McClelland  
Marine Science Institute, University of Texas at Austin,  
Port Aransas, TX, USA

*Present Address:*  
M. Manizza  
Geosciences Research Division, Scripps Institution of  
Oceanography, University of California San Diego,  
La Jolla, CA, USA

Until recently, there has been no cohesive set of measurements of nutrient and organic matter concentrations in the world's major circumpolar rivers. While constituent concentrations in large North American rivers are relatively well documented (Dornblaser and Striegl 2007; Emmerton et al. 2008), those for Eurasian rivers have been periodic or potentially unreliable (e.g., Holmes et al. 2000, 2001). Particularly on Eurasian rivers, constituent measurements have typically been taken during the summer, missing the critical freshet and under ice periods and thus causing lack of a full seasonal coverage (McClelland et al. 2008). The majority of freshwater flux to the Arctic Ocean comes from Eurasia (Lammers et al. 2001), although North American rivers are particle-rich (Holmes et al. 2002; Macdonald et al. 2010). Thus, the lack of a comprehensive Pan-Arctic dataset on riverine biogeochemistry has represented a significant impediment to our understanding of land–ocean coupling in the Arctic.

In response to this gap, the Pan-Arctic River Transport of Nutrients, Organic Matter, and Suspended Sediments (PARTNERS) Project (McClelland et al. 2008) was designed to measure the biogeochemistry of the world's six largest circumpolar rivers—the Ob', Yenisey, Lena, Kolyma, Yukon, and Mackenzie—with samples collected across the full seasonal cycle. Together, these rivers provide more than half of the freshwater flux to the Arctic Ocean and drain a total catchment area of  $10.9 \times 10^6$  km<sup>2</sup> (see Holmes et al. 2011). In a companion piece to this manuscript, nutrient and organic matter concentrations measured during PARTNERS are used to determine the riverine export of these constituents (Holmes et al. 2011). Because of the seasonal coverage and consistent sampling and analytical measurements within the PARTNERS dataset, these represent the best available Pan-Arctic estimates of dissolved nutrient and organic matter flux from rivers to the Arctic Ocean and bring a much greater degree of certainty to our understanding of Pan-Arctic riverine biogeochemistry. Specifically, the dissolved organic nitrogen (DON) fluxes presented in Holmes et al. (2011) are up to two to three times less than previous estimates for the Lena and Kolyma River (Gordeev et al. 1996), but lie within ~20% of a recently estimated budget for the Pan-Arctic which excluded Hudson Bay when the estimates are scaled using discharge (Macdonald et al. 2010). For dissolved inorganic nitrogen (DIN), the new flux estimates from the Ob' and Yenisey River correct previous estimates that are up to an order of magnitude too high as a result of erroneous measurements on these rivers (see Holmes et al. 2000, 2001). We use the improved flux estimates from Holmes et al. (2011) as a starting point to assess the importance of riverine (terrigenous) dissolved inorganic nitrogen (tDIN), dissolved organic nitrogen (tDON), and dissolved organic carbon (tDOC) for primary and bacterial production in the Arctic Ocean.

While inorganic nutrients are directly available for uptake by primary producers, organic nutrients must typically be remineralized to their inorganic forms before they can be assimilated by autotrophs. Organic matter quality ranges from very labile to very recalcitrant (Carlson 2002), allowing terrigenous organic matter to become broadly distributed within the Arctic Ocean before its eventual degradation or export (Amon and Benner 2003; Hansell et al. 2004). A recent modeling effort using a regionally configured version of the MIT general circulation model (MITgcm) successfully reproduced the measured tDOC distribution in the offshore Arctic Ocean (Hansell et al. 2004) by assuming a constant degradation rate for tDOC throughout the ocean basin (Manizza et al. 2009). We build on this work using the Manizza et al. (2009) model to explore the processes that regulate tDON removal from oceanic waters. We assume that the tDOC degradation rate from Manizza et al. (2009) applies to the greater terrigenous dissolved organic matter (tDOM) pool and can thus be used to determine the amount, and spatial distribution, of tDON removal within the Arctic Ocean basin. This assumption is by necessity an imperfect one: first, DOC and DON degradation rates are not equivalent in situ. Second, recent studies indicate that rates of tDOC decay in the Arctic Ocean may follow a multistep process and not follow the constant rate of decay ( $0.1 \text{ year}^{-1}$ ) that the Manizza et al. (2009) model suggests (Alling et al. 2010; Letscher et al. 2011). However, because N-rich DOM is preferentially remineralized within the DOM pool (Sun et al. 1997; Hopkinson et al. 1998; Hopkinson and Vallino 2005), and recent multistep decay functions indicate faster degradation in the nearshore (Letscher et al. 2011), our estimates of tDON removal are likely conservative.

While some of the processes that remove tDON from Arctic surface waters will result in direct N remineralization, others will tend to be an N sink. For example, bacterial consumption of DON can lead either to N sequestration in bacterial biomass or regeneration of DIN, depending on the relative nutrient content of bacteria and the organic matter food source, and the ratio of bacterial growth to respiration (Goldman et al. 1987). Similarly, passage of bacterial biomass through the microbial food web will lead to some N regeneration and some continued sequestration in biomass (Goldman et al. 1985). Non-biological processes, such as photochemical decomposition, also cause the release of DIN from DON (Bushaw et al. 1996).

Here, we rely upon work from previous studies to explore the extent to which tDON that is removed from the water column (hereafter “transformed” tDON) is remineralized as inorganic N. We used this and calculated rates of riverine tDIN flux to assess the potential contribution of riverine nutrients to near- and offshore primary production in the Arctic Ocean. Recently, Macdonald et al. (2010) used

literature estimates to compile shelf-specific budgets that assess the importance of riverine DIN to primary production in the Arctic Ocean. We build on this by specifically exploring the spatial distribution and within-ocean processing of riverine DON and using the updated riverine DIN and DON flux estimates provided in Holmes et al. (2011). This work provides a first approximation of the relative importance of riverine DON and DIN for primary production in the Arctic Ocean and indicates where, spatially, the impact of riverine nutrients should be greatest within the ocean basin. While we expect that future work will refine the estimates that we provide here, this work provides a point of departure for determining future research avenues that will significantly improve our understanding of land–ocean coupling within the Arctic Ocean.

## Materials and Methods

### Sample Collection and Analysis

Nutrient and organic matter concentration data for the estimation of constituent fluxes to the Arctic Ocean were obtained from the PARTNERS dataset, available online through the Cooperative Arctic Data and Information Service (McClelland et al. 2008), and on the Arctic Great Rivers Observatory web site ([www.arcticgreatrivers.org](http://www.arcticgreatrivers.org)). The PARTNERS collection protocol was designed to ensure coverage of base flow (under ice), spring melt, and late summer conditions and followed the same sample collection and analysis methodology on each of the six rivers. PARTNERS data were collected between 2003 and 2006. More information on data collection and sample processing is provided elsewhere (Raymond et al. 2007; McClelland et al. 2008; Holmes et al. 2011).

### Estimating Constituent Flux to the Arctic Ocean

Export of riverine DIN ( $\text{NO}_3$  and  $\text{NH}_4$ ) and DON from the six PARTNERS rivers was estimated using the LoadRunner and LoadEstimator software packages, as described in Holmes et al. (2011). Briefly, the LoadRunner utility (Booth et al. 2007) was used to automate runs of the USGS LoadEstimator program (Runkel et al. 2004). LoadEstimator uses a time series of paired daily stream flow and constituent concentration data to construct a calibration regression that considers factors such as discharge and season, which is then applied to a continuous daily discharge record to obtain estimates of constituent flux. Similarly, estimates of constituent concentration for days without measured concentration data are output from the model. We obtained daily discharge for a 10-year period between 1999 and 2008 from the ArcticRIMS Project

(<http://rims.unh.edu>) for the Eurasian Rivers, the Water Survey of Canada for the Mackenzie River, and the USGS for the Yukon River. Calibration regressions were constructed with PARTNERS constituent data collected between 2003 and 2006, and used to extrapolate fluxes to the 10-year discharge data period to give a decadal mean of yearly constituent flux. For the Yukon River, 1999 and 2000 discharge data were not available, and means of constituent flux are for 2001–2008 only. The calculated yearly DIN flux from the six PARTNERS rivers was used to scale-up to the total DIN flux from the full Pan-Arctic catchment, which includes Hudson, James, and Ungava Bays, by assuming that areal yields in the unmonitored region were equivalent to those from within the PARTNERS catchments, which encompass 53% of the full Pan-Arctic basin (as discussed in Holmes et al. 2011). Given the paucity of data (particularly with respect to seasonal coverage) for estimating DIN fluxes directly for non-PARTNERS arctic rivers, this direct scaling approach is essential to assessing the importance of riverine DIN at the Pan-Arctic scale. We offer two lines of evidence to further support this approach. First, we note that the proportion of continuous plus discontinuous permafrost across the six PARTNERS catchments (48%) is very similar to the proportion within the broader Pan-Arctic catchment (52%; data from the Arctic RIMS Project database). Thus, although riverine dissolved N may vary across latitudinal and permafrost gradients (reviewed in Frey and McClelland 2009), the PARTNERS watershed region appears to be representative of the Pan-Arctic as a whole. Second, individual PARTNERS watersheds vary from fully Arctic and within the zone of continuous permafrost to nearly permafrost-free and thus capture this range of variability that occurs across the full Pan-Arctic. For example, the range of DIN yields from PARTNERS rivers (13–31  $\text{mg m}^{-2}$ ; Holmes et al. 2011) overlaps the combined yield from a series of three small, wholly Arctic rivers from the Alaskan north slope (16  $\text{mg m}^{-2}$ ; McClelland et al. 2011a).

### Assessing the Importance of Riverine Inorganic Nutrients to the Nearshore

We compared concentrations of riverine DIN and Si to measured oceanic concentrations to examine the effect of riverine inorganic nutrients on the nearshore zone. Riverine nutrient concentrations were taken from the LoadEstimator output using flow-weighted concentrations from the output presented in Holmes et al. (2011). Oceanic nutrient concentrations were taken from published estimates of the bottom of the mixed layer for the Laptev and Beaufort Seas (Dittmar et al. 2001; Carmack et al. 2004; Simpson et al. 2008). To examine how these nutrients might affect production in the nearshore zone, we constructed theoret-

ical mixing curves using these nutrient concentrations as the zero- and high-salinity end-members.

### Assessing the Importance of Riverine DON over Arctic Shelves and the Open Ocean

Estimates of within-ocean tDON transformation were obtained using the MITgcm (Marshall et al. 1997), as described in Manizza et al. (2009). We used the DOC e-folding lifetime of 10 years from Manizza et al. (2009) to assess DON decay and calculated the input of tDON from land to the Arctic Ocean by rescaling the DOC fluxes from Manizza et al. (2009) using the C/N ratio for dissolved organic matter observed from the six PARTNERS rivers (~50, mol/mol; standard error=1.3). The model is configured on a “cubed-sphere” grid in a limited area Arctic domain with open boundaries at ~55° N in the Atlantic and Pacific sectors. Prescribed boundary conditions for potential temperature, salinity, flow, and sea surface elevation are provided from previous integrations of a global configuration of the same model (Menemenlis et al. 2005). The grid is locally orthogonal and has a variable horizontal resolution with an average spacing of ~18 km. The mesh resolves major Arctic straits, including many of the channels of the Canadian Archipelago. This model configuration was used to study the Arctic freshwater budget (Condrón et al. 2009) previous to the study of tDOC distribution (Manizza et al. 2009). The sea ice and fluid dynamical equations are solved on the same horizontal mesh. The vertical grid is height-based, varying from 10-m-thick near the surface to ~450 m at a depth of ~6 km in 28 levels. Bathymetry is derived from the U.S. National Geophysical Data Center 2-min global relief dataset (ETOPO2), which uses the International Bathymetric Chart of the Arctic Ocean product for Arctic bathymetry. An extensive technical description of the model used to generate the surface Arctic fields of tDOC is given in Manizza et al. (2009).

Yearly rates of tDON transformation were derived from the model by applying the Manizza et al. (2009) degradation rate to the modeled tDON distribution from the oceanic surface layer (top 10 m) in the MITgcm. In recognition of the fact that the Arctic Ocean mixed layer depth is deeper than 10 m (15–20 m in the spring–summer; McLaughlin et al. 2005), we also discuss tDON transformation estimates corrected to a mixed layer depth of 20 m to provide consistency with other primary production estimates (Walsh et al. 2005; Pabi et al. 2008). In accordance with the configuration of the Arctic domain MITgcm and the river flux manuscript by Holmes et al. (2011), we defined the geographic extent of the Arctic Ocean using the International Hydrographic Organization boundaries (Jakobsson 2002), which include Hudson Bay, Hudson Strait, and the Canadian Archipelago. To determine the relative spatial

importance of tDON transformation, we demarcated our defined Arctic Ocean between the open ocean, where depth to bottom is >200 m, and shelves, with depth to bottom <200 m (Fig. 1).

### Estimates of DIN Regeneration from tDON Transformation

We assume that oceanic transformation of tDON occurs as a result of both biological and photochemical processes. To examine the fate of transformed tDON over shelves and the open ocean, we estimated rates of photoammonification and bacterial DIN regeneration and explored the extent to which DIN is likely to be regenerated at higher trophic levels within the microbial food web (e.g., Goldman et al. 1985).

#### tDON Decomposition by Photoammonification

Photoammonification in the top 10 m of ocean was calculated following Vähätalo and Zepp (2005) and Bélanger et al. (2006) as:

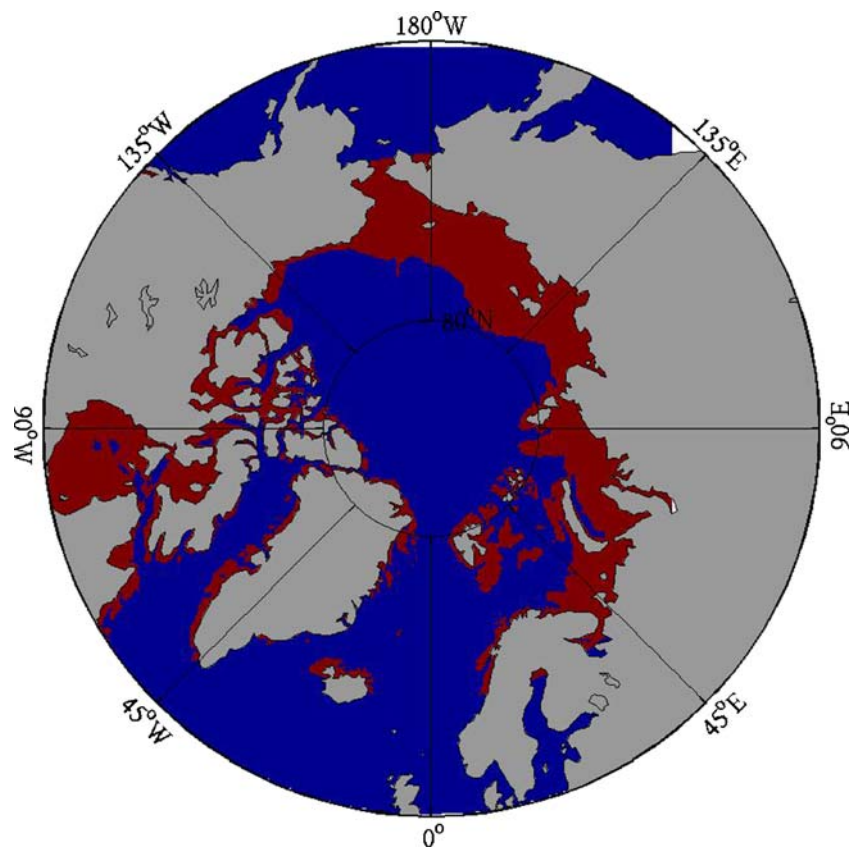
$$P_{\text{NH}_4} = \int_{\lambda_{280}}^{\lambda_{650}} \Phi_{\text{NH}_4,\lambda} \cdot E_d(0^-, \lambda) \cdot \frac{a_{\text{tDOM},\lambda}}{a_{\text{tot},\lambda}} (1 - \text{trans}_\lambda) d\lambda$$

where  $P_{\text{NH}_4}$  is the depth-integrated rate of  $\text{NH}_4$  photoproduction ( $\text{mol N m}^{-2} \text{d}^{-1}$ ),  $\Phi_{\text{NH}_4,\lambda}$  is the apparent quantum yield (AQY) for photoammonification [ $\text{mol N (mol photons)}^{-1} \text{nm}^{-1}$ ],  $E_d(0^-, \lambda)$  is the downward irradiance just below the water's surface ( $\text{mol photons m}^{-2} \text{day}^{-1} \text{nm}^{-1}$ ),  $a_{\text{tDOM},\lambda}/a_{\text{tot},\lambda}$  (dimensionless) is the proportional contribution of riverine DOM to the total absorption coefficient (i.e., absorption by tDOM, marine DOM, seawater, and particles), and  $\text{trans}_\lambda$  is the proportion of downward irradiance transmitted through the top 10 m of ocean.

Curves for  $\Phi_{\text{NH}_4,\lambda}$  were obtained from a series of literature estimates of photoammonification on river, estuarine, and seawater (Bushaw et al. 1996; Vähätalo and Zepp 2005; Stedmon et al. 2007). Downward irradiance was estimated using the U.S. National Renewable Energy Laboratory's SMARTS model (Simple Model of the Atmospheric Radiative Transfer of Sunshine; Gueymard 2001, 2006). We used the arctic summer atmosphere to calculate water vapor, ozone, and carbon dioxide and assumed a maritime aerosol environment, with turbidity levels as measured by Stone et al. (2008). We used a fixed albedo of 0.05, as previously measured for water (e.g., Bélanger et al. 2006). Total daily irradiance at 71.25° N, the mean latitude of the entry point of the six PARTNERS rivers into the Arctic Ocean, was calculated at weekly intervals by obtaining hourly irradiance outputs from the model and integrating over the day of interest. The cloud-free daily downward irradiance output by the model was



**Fig. 1** The Arctic Ocean split into shelf (<200 m, red) and open ocean (>200 m, blue) domains



corrected by 0.70, to adjust for average cloud conditions at this latitude (Frederick and Lubin 1988), and 0.95, to account for reflection at the water surface and obtain  $E_d(0^-, \lambda)$  (Bélanger et al. 2006).  $a_{tDOM}$  was calculated using the flow-weighted absorption coefficient at 375 nm ( $a_{375}$ ) measured for the six PARTNERS rivers, normalized to 1.2  $\mu\text{M}$ , the concentration at which the tDON plume experiences a sharp drop-off in oceanic waters (60  $\mu\text{M}$  tDOC; Manizza et al. 2011). Because these are minimum concentrations taken from the outer edge of the tDOM plume, our calculated  $a_{tDOM}$  likely underestimates the true absorption by riverine DOM. tDOM absorption estimates were expanded to the full spectrum of interest using flow-weighted average spectral slopes ( $S_{300-650}$ , wavelength range of 300–650 nm) calculated for PARTNERS rivers (Stedmon et al. 2011). The absorbance of marine-derived DOM ( $a_{mDOM}$ ) was calculated based on  $a_{375}$  and  $S_{300-650}$  values given for Arctic surface water in Stedmon and Markager (2001). Absorption by particulates and seawater ( $a_{part}$ ) was estimated using measured fractional absorbances for North American shelf waters ( $a_{CDOM}/a_{tot}$ ; Bélanger et al. 2006) using the sum of  $a_{tDOM}$  and  $a_{mDOM}$  for  $a_{CDOM}$ . The three absorption coefficients ( $a_{tDOM}$ ,  $a_{mDOM}$ , and  $a_{part}$ ) were used to calculate absorption in our 10-m zone of interest; all remaining incident radiation was assumed to pass through this zone unabsorbed (i.e.,  $\text{trans}_\lambda$ ).

#### Biological Regeneration of $\text{NH}_4$ from tDON

We assumed that all transformed tDON not subject to photodecomposition is taken up by bacteria and used the approach of Goldman et al. (1987) to calculate potential bacterial regeneration of  $\text{NH}_4$  from tDON as:

$$E_N = C_T \left( \frac{1}{C/N_{DOM}} - \frac{\text{BGE}}{C/N_{bact}} \right),$$

where  $E_N$  is the rate of  $\text{NH}_4$  regeneration ( $\text{mol time}^{-1}$ ),  $C_T$  is the rate of C uptake by bacteria ( $\text{mol time}^{-1}$ ),  $C/N_{DOM}$  and  $C/N_{bact}$  are the molar C/N ratios of the DOM substrate and bacteria, respectively, and BGE is bacterial growth efficiency; the proportion of bacterial C uptake is apportioned to biomass creation (BGE = bacterial production/[bacterial production + bacterial respiration]).

To assess the potential range of bacterial  $\text{NH}_4$  regeneration, we used BGEs ranging from a low of 0.1, similar to growth efficiencies measured on the Chukchi and Beaufort shelves (Kirchman et al. 2009) and for Mackenzie River floodwater (Tank 2009), to a high of 0.27, measured in the nearshore Kara Sea (Meon and Amon 2004), and molar bacterial C/N ratios ranging from 4 to 6.7 (Goldman et al. 1987). The C/N for tDOM was held constant at the average

ratio observed from the six PARTNERS rivers (50, mol/mol, described previously).

Laboratory-based studies suggest that protozoans have high rates of N regeneration, with each trophic step within the microbial web resulting in ~50% remineralization (Goldman et al. 1985). Thus, all tDON incorporated into bacterial biomass was allowed to pass to higher trophic levels within the microbial loop, where we assign a 50% regeneration rate with each trophic step.

#### Calculating Productivity Derived from Riverine Nutrients and Organic Matter

Primary production was calculated using a stoichiometric conversion of inorganic N to C (molar C/N=6.625). We assume that all tDIN, and all tDON regenerated as DIN in the surface layer of the ocean shelf, is fully used by phytoplankton in the spring bloom. Bacterial production was also calculated by estimating oceanic tDOC degradation rates as for tDON and partitioning yearly tDOC degradation between bacterial production, bacterial respiration, and the photoproduction of inorganic carbon (Bélanger et al. 2006). We use previously measured BGEs to calculate the magnitude of bacterial production relative to bacterial respiration (Meon and Amon 2004; Kirchman et al. 2009; Tank 2009) and assumed that DIC photoproduction was 10% the rate of bacterial respiration (see Bélanger et al. 2006).

## Results

### Inorganic Nutrient Inputs from Large Arctic Rivers to the Arctic Ocean

A detailed analysis of riverine nutrient flux to the Arctic Ocean is provided by Holmes et al. (2011). Briefly, the six largest arctic rivers discharge an estimated 16.3 Gmol (229 Gg) year<sup>-1</sup> of DIN to the Arctic Ocean, 13.0 Gmol (182 Gg) of which is exported as NO<sub>3</sub> (Holmes et al. 2011). In the Yenisey, Yukon, and Mackenzie Rivers, NO<sub>3</sub> is >90% of the DIN export, while NH<sub>4</sub> contributes more substantially to DIN export from the Kolyma, Lena, and Ob' Rivers (24%, 28%, and 34% of DIN exported as NH<sub>4</sub>, respectively). DIN export extrapolated to the Arctic Ocean as a whole equals 30.7 Gmol (430 Gg) year<sup>-1</sup>. Flow-weighted averages of DIN concentration in large Eurasian rivers range from 4 to 14 μM, while concentrations in large North American rivers range from 6 to 9 μM (Fig. 2). Yearly Si flux from the six largest Arctic rivers totals 216 Gmol (6,062 Gg), and flow-weighted concentrations range from 66 to 121 μM (Holmes et al. 2011; Fig. 2).

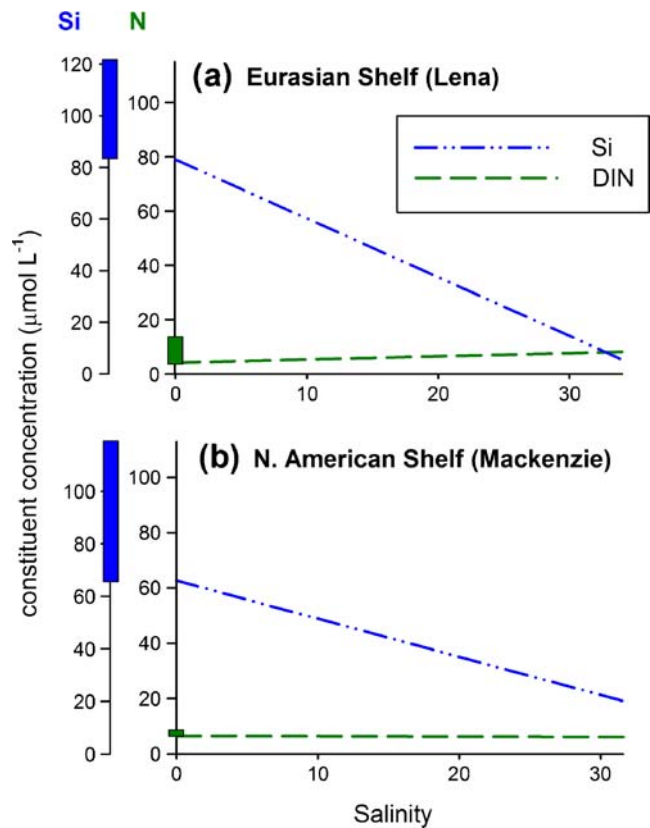


**Fig. 2** Theoretical mixing curves for dissolved inorganic nitrogen (DIN) and Si over the Eurasian and North American shelves. Zero-salinity end-members are flow-weighted average concentrations from the Lena (a) and Mackenzie (b) Rivers. High-salinity end-members are measured concentrations from the bottom of the mixed layer in the Laptev (a) and Beaufort (b) Seas (Dittmar et al. 2001; Carmack et al. 2004; Simpson et al. 2008). For comparison, the range of PARTNERS flow-weighted DIN and Si concentrations for Eurasian (a) and North American (b) rivers is indicated by shaded bars on the y-axis. The y-axes are scaled to the Brzezinski ratio for Si/N (1.05; Brzezinski 1985) such that the lower-lying curve indicates the limiting nutrient

While riverine concentrations of Si are always well in excess of winter maximum concentrations found in the Arctic Ocean mixed layer, riverine DIN either dilutes or is similar in concentration to oceanic DIN (Fig. 2). In all rivers, ratios of Si/N are well above the Redfield–Brzezinski ratio of ~1 (Fig. 2). This is also true for winter mixed layer maximum concentrations from the Beaufort Shelf, resulting in a theoretical mixing curve for the Mackenzie River outflow that is Si-rich across the full range of salinities (Fig. 2). On the Laptev Shelf, the winter maximum Si/N ratio is slightly <1, which gives a theoretical mixing curve that is Si-rich at all but the highest salinities (Fig. 2). Because concentrations of riverine nutrients are relatively similar across the PARTNERS rivers, this trend holds for each of these six largest north-flowing rivers (Fig. 2).

## Modeled Transformation of tDON in the Arctic Ocean

The total flux of tDON from the six PARTNERS rivers is 32.1 Gmol (450 Gg) year<sup>-1</sup> (Holmes et al. 2011). Based on a direct scaling from the estimates of Pan-Arctic tDOC flux in Manizza et al. (2009), the total export of tDON to the Arctic Ocean is 53.8 Gmol year<sup>-1</sup>, estimated for the ten Pan-Arctic domains outlined in Lammers et al. (2001) and Manizza et al. (2009). Fully half of the Pan-Arctic tDON export is to the Kara and Laptev Seas. At steady state, and given the e-folding decomposition rate of 10 years from Manizza et al. (2009), the modeled tDON distribution covers a large proportion of the Eurasian shelf, forms a considerable plume at the outflow of the Mackenzie River, and spreads well into the open ocean in several areas. This leads to rates of tDON transformation with a similarly broad distribution (Fig. 3). In total, 13.6 Gmol year<sup>-1</sup> of tDON is transformed in the top 10 m of the Arctic Ocean, or 27.1 Gmol year<sup>-1</sup> if estimates are extrapolated to a mixing depth of 20 m. The majority of tDON transformation occurs over shelf regions (11.5 Gmol year<sup>-1</sup> over the 10-m surface layer of the MITgcm), with much lower rates in the open ocean (2.1 Gmol year<sup>-1</sup>; Fig. 3). The highest areal rates of surface tDON transformation are found in the nearshore regions of the Kara, Laptev, East Siberian, and Beaufort Seas, where modeled rates peak near 3 μmol L<sup>-1</sup> year<sup>-1</sup>. An analysis of how variability in the DOM degradation rate might affect tDON transformation is provided in the “Discussion.”

### Regeneration of tDON to NH<sub>4</sub>

To better understand the fate of tDON transformed in the Arctic Ocean, we estimated the rate of NH<sub>4</sub> regeneration from tDON by photodecomposition, bacterial metabolism, and excretion by grazers within the microbial food web. Published AQY curves for ammonium production from DON show a wide possible range for photoammonification quantum yield, representing environments from freshwater to the open ocean (Fig. 4a). For the calculations that follow, we chose a curve produced from nearshore oceanic waters heavily influenced by the inputs of terrigenous DOM (Stedmon et al. 2007, highlighted in Fig. 4a). Photoammonification is most efficient at lower wavelengths, where absorption by tDOM also dominates (Fig. 4b). Thus, 90% of our estimated tDON photoammonification is accomplished by wavelengths <415 nm (Fig. 4c). Daily rates of potential NH<sub>4</sub> photoproduction peak during summer solstice, when NH<sub>4</sub> regeneration is estimated at 43 μmol N m<sup>-2</sup> day<sup>-1</sup> (Fig. 4d), given our assumed normalized absorbance at 1.2 μM tDON (see “Materials and Methods”).

In contrast, the modeled ice-free area of the tDOM plume is greatest in September, consistent with the well-

known yearly arctic sea ice minimum (Fig. 4d). By this time, areal rates of photoammonification have declined significantly due to declining levels of solar radiation. As a result of this offset between peak radiation and open water area, modeled photoammonification across the arctic as a whole peaks in late summer (Fig. 4e). Total estimated photoammonification over the summer melting season is 2.6 Gmol N, or 19% of the yearly tDON transformation in the top 10 m of the ocean. In regions that remain ice-free between July 1 and the end of September, aerial photoammonification rates are 2.4 mmol N m<sup>-2</sup> year<sup>-1</sup>. Our chosen AQY curve was specifically selected for its representation of nearshore tDOM-influenced environments. However, across the full range of AQY curves represented in Fig. 4a, calculated photoammonification rates range by almost an order of magnitude (data not shown).

Rates of bacterial N regeneration calculated over a realistic range of BGEs (0.10–0.27) and bacterial C/N ratios (4–6.7, mol/mol) demonstrate that at all but the lowest BGEs (<0.134) and moderate and greater bacterial C/N ratios (>5), bacteria sequester, rather than regenerate, N. When BGE is 0.1 and bacterial C/N is 6.7, bacteria regenerate 25.4% of the N that they consume, the maximum rate given our range of scenarios. To estimate the full range of potential tDON regeneration, we allow photoammonification to proceed over oceanic shelves as modeled above, bacterial N regeneration to range from 0% to 25.4%, and the number of trophic steps in the microbial food web that occur before biologically sequestered N falls out of the mixed layer to range from 1 to 2. Of the tDON transformed in the top 10 m of ocean, 59–85% is regenerated given this range of scenarios, or 8.1–11.5 Gmol N year<sup>-1</sup> over both shelf and open ocean regions. Extending these calculations to tDON transformed in the top 20 m of ocean results in N regeneration between 55% and 83%, or 14.8–22.5 Gmol N year<sup>-1</sup>. Figure 5 gives a schematic diagram that illustrates our N regeneration estimates, split over shelf and open ocean areas.

### Riverine Nutrients and Organic Matter as a Substrate for Primary and Bacterial Production

We use the flux of tDIN and our estimates for DIN directly regenerated from tDON to calculate potential rates of what we term “initial” primary production, that is, productivity that results from the initial uptake of riverine N by oceanic phytoplankton. These estimates explicitly exclude subsequent recycling of N that will occur within the pelagic zone, which is further explored in the “Discussion” below. Assuming Redfield rates of N/C conversion, the 30.7 Gmol of tDIN that flows to the Arctic Ocean each year could support initial primary production of roughly 200 Gmol C year<sup>-1</sup>. Similarly,

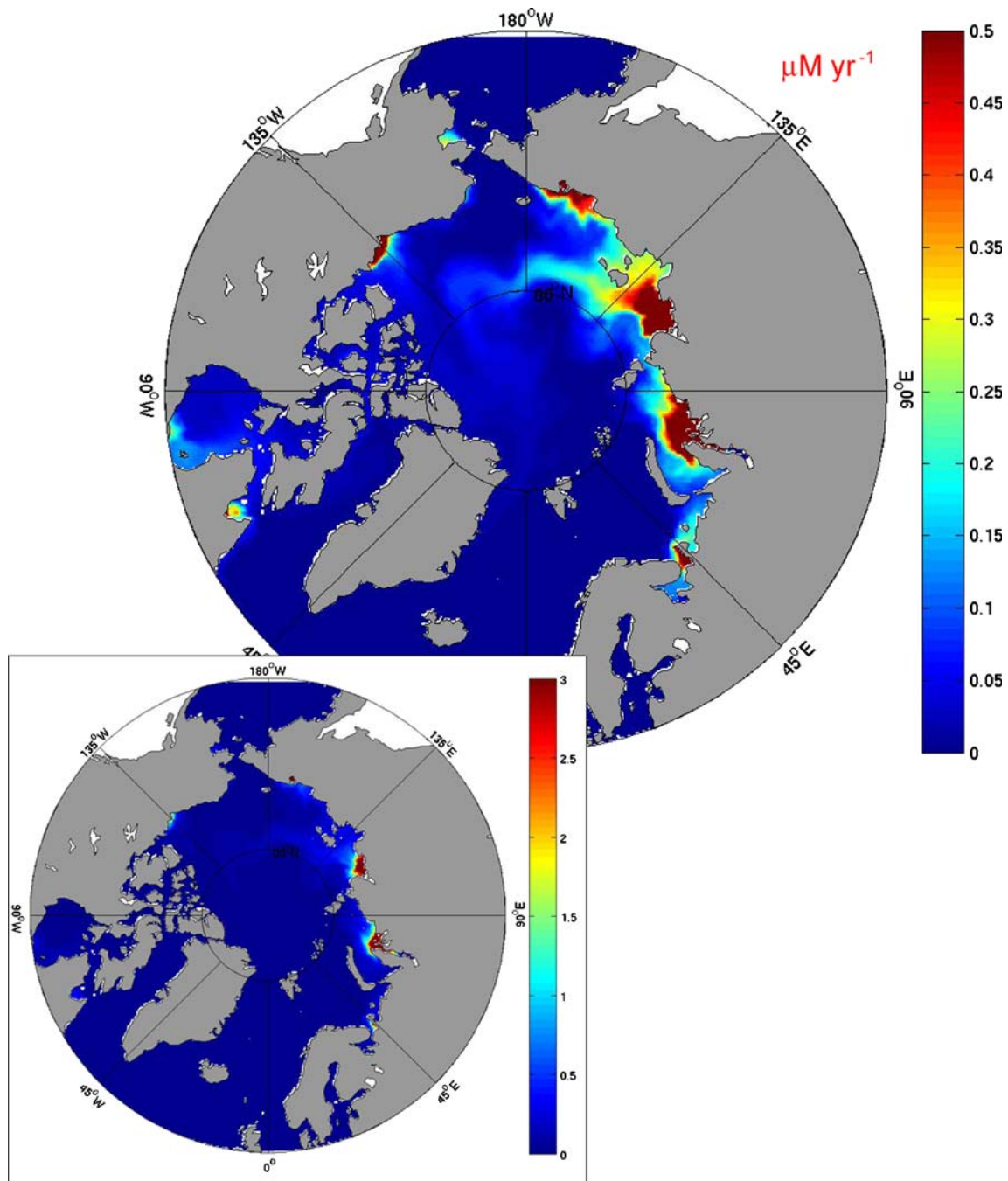


**Fig. 3** Yearly tDON transformation rates for the top 10 m of the Arctic Ocean, modeled using the MITgcm. The main figure is scaled between 0 and 0.5  $\mu\text{M year}^{-1}$  to show the extensive distribution of

tDON in the Arctic Ocean. The *inset* is scaled between 0 and 3  $\mu\text{M year}^{-1}$  to show peak transformation rates

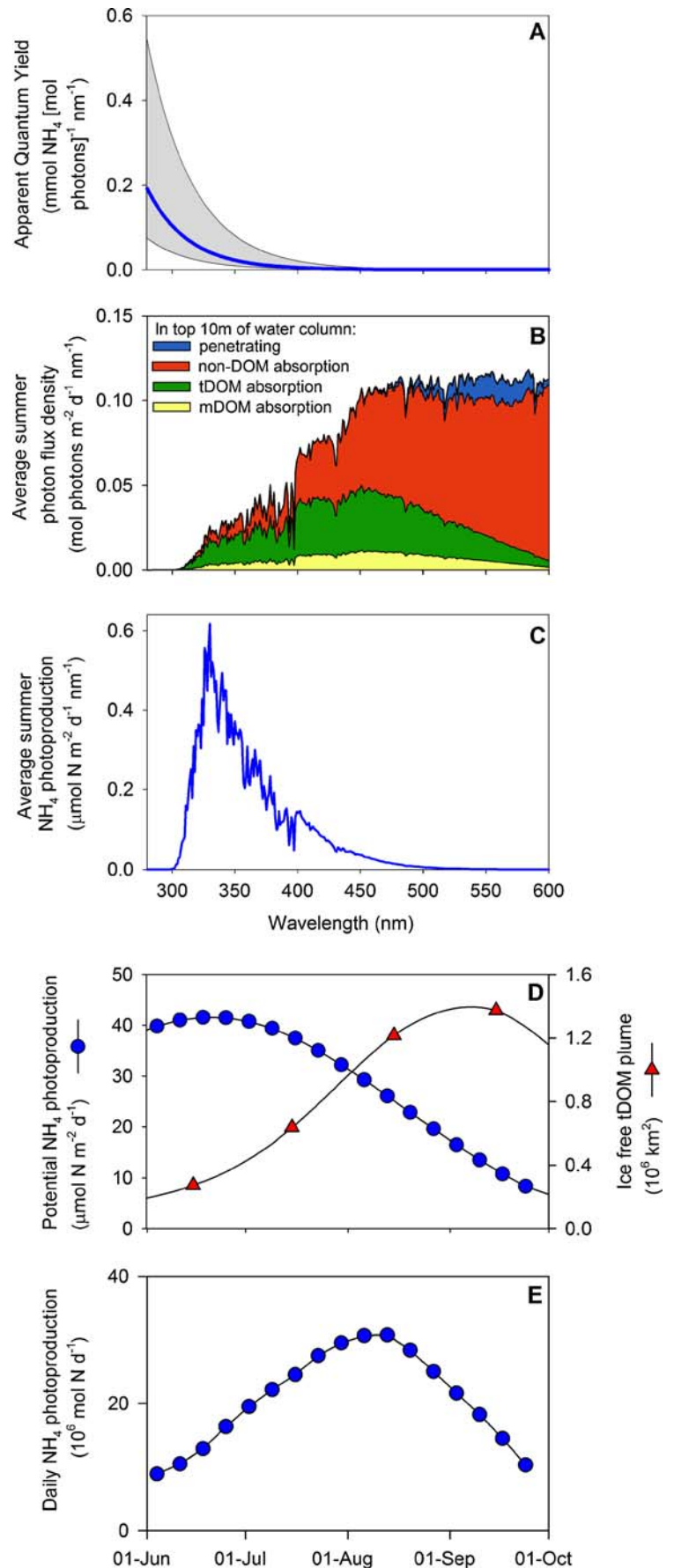
the range of potential tDON regeneration over the top 20 m of ocean could support initial primary production ranging from 98 to 149  $\text{Gmol C year}^{-1}$ . Given the spatial distribution of tDON regeneration (Fig. 5), this would be split between shelf (85–127  $\text{Gmol C year}^{-1}$ ) and open ocean (14–22  $\text{Gmol C year}^{-1}$ ) regions. However, given that N is not necessarily limiting under ice, complete utilization of

regenerated tDON for primary production may not occur in open ocean regions (Gosselin et al. 1997).

On an areal basis, tDON transformation in nearshore regions reaches 3  $\mu\text{M year}^{-1}$ , which could sustain initial primary production over the top 20 m of ocean ranging from 0.2 to 0.3  $\text{mol C m}^{-2} \text{ year}^{-1}$ . tDIN-supported primary production in the nearshore, however, should be much more



**Fig. 4** Photoammonification estimates for tDON in the top 10 m of the Arctic Ocean. A known apparent quantum yield (AQY) for photoammonification (Stedmon et al. 2007 (a)) was multiplied by downwelling radiation absorbed by riverine dissolved organic matter (tDOM) (b) to obtain potential rates of NH<sub>4</sub> photoproduction (c). Weekly potential photoproduction rates were multiplied by the ice-free area of the tDOM plume (d) to calculate in situ NH<sub>4</sub> photoproduction (e). In b, downwelling radiation is partitioned between penetration through the 10-m surface layer and absorption by tDON, marine DOM (mDOM), and constituents in the water column other than DOM (non-DOM). In a, the blue line indicates the chosen AQY curve; the gray shading indicates a range of published AQY curves from across various environments



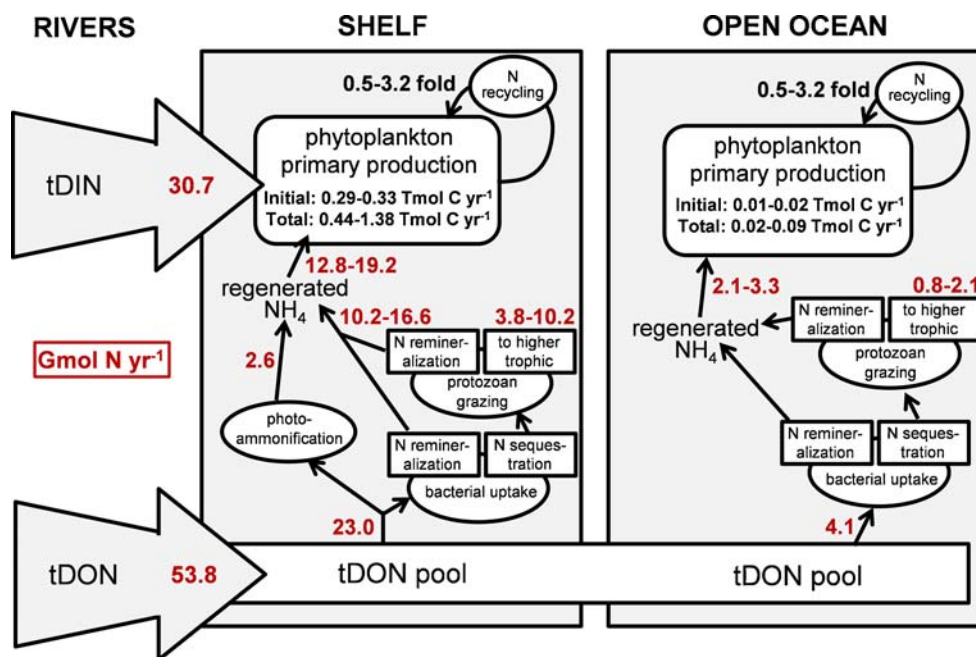


**Fig. 5** Conceptual diagram showing tDIN and tDON inputs to the Arctic Ocean and their impact on oceanic primary production. Rates of tDON regeneration as DIN were modeled for the top 10 m of ocean using the MITgcm and directly scaled to an estimated 20-m mixing depth. Primary production supported by riverine nutrients over

oceanic shelves and the open ocean is shown. Units in red are gigamoles N per year and units in black are teramoles C per year, as noted. Primary production is not necessarily nutrient-limited under ice cover, and thus open ocean productivity values should be taken as maximum possible estimates

concentrated as a result of rapid uptake of this limiting nutrient. For example, if we assume that the  $9.7 \text{ Gmol year}^{-1}$  of tDIN discharged from the Yenisey and Ob' Rivers is taken up in the nearshore region of the Kara Sea ( $\sim 70,000 \text{ km}^2$ ; Frey et al. 2007), average levels of initial primary production of  $\sim 0.9 \text{ mol C m}^2 \text{ year}^{-1}$  would result.

Of tDOC, 0.68 Tmol is degraded in the top 10 m of the Arctic Ocean each year, given the degradation rates from Manizza et al. (2009). If this pool of riverine C is partitioned between bacterial production, bacterial respiration, and direct photodegradation, rates of bacterial production ranging from 60 to  $170 \text{ Gmol C year}^{-1}$  result ( $120\text{--}340 \text{ Gmol C year}^{-1}$  if estimates are extended to 20 m), depending on the growth efficiency of bacteria on the C substrate (Meon and Amon 2004; Kirchman et al. 2009; Tank 2009).

## Discussion

Theoretical N/Si mixing curves constructed for Arctic estuarine gradients demonstrate that Si is generally in excess throughout nearshore regions and that diatom production should typically be N, rather than Si, limited where light conditions permit (see also Dittmar et al. 2001; Simpson et al. 2008; Tremblay and Gagnon 2009). The lack of direct inorganic P measurements for the PARTNERS

estuaries precludes a detailed assessment of N vs. P limitation for overall primary production in the Arctic nearshore. However, measurements of inorganic N and P by other authors have shown Mackenzie river water to be P-limited, both during the spring freshet (molar N/P $\sim$ 20) and thereafter (Emmertson et al. 2008). In contrast, late summer point measurements of inorganic N and P from Russian rivers indicate potential N limitation (Dittmar et al. 2001). Measurements from the Arctic Ocean show N to be the primary limiting nutrient further offshore (Dittmar et al. 2001; Simpson et al. 2008). The indicated gradient from P to N limitation in the Beaufort Sea has been observed: while there is evidence for P limitation in the inner Mackenzie Shelf (Carmack et al. 2004), near-complete summertime inorganic N consumption occurs as salinities rise slightly (Carmack et al. 2004; Simpson et al. 2008). Conversely, rapid summertime depletion of  $\text{NO}_3$  across the full estuarine gradient in the Laptev Sea indicates N limitation throughout this Eurasian shelf region (Kattner et al. 1999).

This strong evidence for N limitation indicates that tDIN, and tDON regenerated as  $\text{NH}_4$ , should be rapidly taken up when and where light conditions permit. This, in turn, will lead to strong spatial and temporal dichotomies in the importance of tDIN and tDON in the Arctic Ocean. For tDIN, uptake should largely be limited to nearshore regions. Riverine fluxes of tDIN during winter may be trapped by

the ice dams that occur over shelves at the convergence of land-fast and drifting ice (Macdonald et al. 2004). This, and subsequent riverine tDIN flux during higher flow periods in the spring and summer, should be fully consumed by the annual phytoplankton bloom as the ice edge recedes. In contrast, uptake of tDON-derived N will be much more dispersed. tDON-derived N becomes available for uptake in regions well beyond the immediate nearshore (Fig. 3) and in a manner that is much more smoothly spread across seasons (modeling results, data not shown). Consequently, tDON-derived N is more likely to contribute to widely distributed processes such as the growth of ice algae. Beyond the immediate nearshore regions, the influx of N to the greater Arctic Ocean from the Bering and Barents Sea, and through upwelling is large (Macdonald et al. 2010). Thus, the wide distribution of tDON transformation will often occur in regions where riverine N composes a much smaller proportion of the overall nutrient pool, and—beyond the ice edge—in areas where nutrients may no longer limit productivity.

Although the model by Manizza et al. (2009) provides an excellent fit to measured concentrations of DOC in both the eastern and western Arctic, more recent work suggests that tDOM degradation may proceed even more rapidly over shelves than the Manizza et al. (2009) model indicates, with tDOM degradation rates varying as water passes from river mouths to the open ocean (Alling et al. 2010; Letscher et al. 2011). In this work, we scale the MITgcm output for the top 10 m of ocean to an assumed 20-m mixing depth (McLaughlin et al. 2005). This results in a 43% DON loss over shelves (Fig. 5), consistent with a 5-year integrated shelf residence time at the modeled 0.1-year<sup>-1</sup> degradation rate. This residence time is at the high end for current Eurasian shelf estimates (Letscher et al. 2011). If we were to assume the average estimated Eurasian shelf residence time of 3.5 years (Letscher et al. 2011), a 0.1-year<sup>-1</sup> degradation rate would indicate a 30% DON loss over shelves, which would be consistent with extrapolating our model outputs to a 15-m mixing depth. Our assumed 20-m mixing depth was chosen to allow for comparisons with Pan-Arctic estimates of primary production that were calculated over similar depths (Pabi et al. 2008). However, the calculations above can also provide a useful comparison point against the recent measurements by Alling et al. (2010) and Letscher et al. (2011), which indicate that ~50% of tDOC could be degraded during transit over the broad Eurasian shelves, with nearshore degradation rates up to 0.3 year<sup>-1</sup>. Although our estimates of nearshore tDON degradation may be conservative, it seems clear that tDON becomes widely distributed over the broad shelves of the eastern Arctic, travels off shelves to the open ocean, and is able to act as a “slow-release” nutrient throughout the ocean basin.

In addition to the “initial” production that we calculate, both tDIN and tDON will be recycled within the Arctic Ocean after being taken up by phytoplankton. Estimates of nutrient recycling (i.e.,  $f$  ratios; Eppley and Peterson 1979) are relatively scarce for the Arctic. Many of the estimates that do exist were calculated for the north and northeast water polynas, areas where total annual productivity is similar to those seen in riverine-influenced nearshore zones of the Arctic (Pabi et al. 2008).  $F$  ratio estimates for these regions range from 0.24 to 0.65, giving estimates for the number of times a nutrient is recycled within the euphotic zone ( $[1 - f]/f$ ) of 0.5–3.2 (Smith et al. 1997; Tremblay et al. 2006; Garneau et al. 2007). Within this range, the higher  $f$  ratios and lower recycling rates are from calculations performed over the full arctic bloom cycle, while the lower  $f$  ratios are for point estimates during secondary, late summer blooms. Applying these recycling rates increases our estimate of yearly productivity that could be supported by riverine nutrients, assuming a 20-m mixing depth. For tDIN, initial productivity rates of 200 Gmol C year<sup>-1</sup> (or, nearshore 0.9 mol C m<sup>-2</sup> year<sup>-1</sup>) increase to total rates ranging from 310 to 850 Gmol C year<sup>-1</sup> and nearshore areal rates ranging from 1.4 to 3.8 mol C m<sup>-2</sup> year<sup>-1</sup>. For tDON-derived N over oceanic shelves, initial productivity rates of 85–127 Gmol C year<sup>-1</sup> (or nearshore 0.2–0.3 mol C m<sup>-2</sup> year<sup>-1</sup>) increase to total rates ranging from 130 to 530 Gmol C year<sup>-1</sup> and nearshore areal rates ranging from 0.3 to 1.4 mol C m<sup>-2</sup> year<sup>-1</sup>. The effect of recycling on the rates of total primary production is detailed in Fig. 5.

In addition to supporting primary production, riverine nutrients and organic matter also support new bacterial production. Surface rates of riverine-supported bacterial and primary production are similar to one another. Assuming a 20-m mixing depth, we calculate that tDOC could directly support 120–340 Gmol of bacterial production per year, while the uptake of tDIN and regenerated tDON could support initial primary production of 200 and 98–149 Gmol C year<sup>-1</sup>, respectively. Like primary production, bacterial production can be expected to support food web processes, directly offering support to the microbial food web and indirectly to higher trophic levels. Despite their similar magnitude, however, the importance of bacterial production to higher trophic levels in the Arctic Ocean is likely much lower than algal production: the greater number of trophic linkages in bacterially based food webs typically results in decreased energy flow to higher trophic levels (~10-fold; Berglund et al. 2007).

In calculating our productivity estimates, we assume that biological uptake of tDON occurs solely by bacteria and that of tDIN solely by algae. This is likely incorrect. Bacterial competition for inorganic N has been well documented (e.g., Kirchman 1994) and shown to suppress phytoplankton biomass (Joint et al. 2002). This competition

has also been observed in the Arctic. In Barents Sea surface waters, bacteria accounted for 17% of both  $\text{NH}_4$  and  $\text{NO}_3$  uptake (Allen et al. 2002). In Arctic polynya waters, even when phytoplankton were relatively abundant (chlorophyll  $a > 2 \mu\text{g L}^{-1}$ ), heterotrophic bacteria accounted for 38% of  $\text{NO}_3$  uptake and 61% of  $\text{NH}_4$  uptake (Fouilland et al. 2007). Conversely, however, the uptake of small, labile DON molecules by algae is also well known, either directly, after cleavage by extracellular enzymes, or as a result of tDON photolysis, which releases small organic molecules in addition to  $\text{NH}_4$  (reviewed in Bronk et al. 2007). Previous work in other systems has estimated that as much as 20% of DON use occurs as a result of phytoplankton uptake after cleavage by extracellular enzymes (Mulholland et al. 1998) and that the uptake of simple DON molecules can supply as much as 80% of phytoplankton N uptake in coastal systems (Bronk et al. 2007). In the Arctic nearshore, both bacterial uptake of tDIN and direct algal consumption of tDON seem likely. Our estimates of bacterial  $\text{NH}_4$  generation from tDON show that over a wide range of possible scenarios, bacteria sequester, rather than regenerate, N. This strongly suggests that—in some situations at least—Arctic oceanic bacteria will supplement their DON uptake with DIN. Conversely, Si and inorganic P concentrations are known to decline in the Arctic nearshore after DIN has disappeared, suggesting utilization of a non-inorganic N source for primary production (Simpson et al. 2008; Tremblay and Gagnon 2009). While some of the N is likely supplied by photoammonification, direct algal uptake of labile DON is also indicated. Thus, algal uptake of DON and bacterial uptake of DIN can be expected to offset each other to some extent, and the exact effect of these processes on our productivity estimates is difficult to determine.

The extremely high spring freshet discharge that is characteristic of these north-flowing rivers cause flood water to move off-channel into river-mouth deltas during the peak flow period and be slowly discharged during the falling limb of the hydrograph (Walker 1998; Emmerton et al. 2008). This occurs to a greater or lesser extent depending on specific river hydrology and river-mouth floodplain topography: while the river-mouth deltas on most of the PARTNERS rivers are relatively small ( $3.0\text{--}4.0 \times 10^3 \text{ km}^2$ ), those of the Mackenzie ( $13 \times 10^3 \text{ km}^2$ ) and Lena ( $32 \times 10^3 \text{ km}^2$ ) have greater water storage capacities (Walker 1998). Water stored off-channel can undergo increased biological activity as particles settle out of suspension and water slows and warms, which, in turn, could alter constituent concentrations. However, PARTNERS measurements are undertaken immediately upstream of these river-mouth deltas because of the logistical constraints that they present.

The effect of delta water storage has been best studied in the Mackenzie River, where it has been shown to decrease

concentrations of inorganic nutrients and increase organics. Emmerton et al. (2008) estimate that the falling limb flux of DIN decreases by 13% as a result of passage through the Mackenzie Delta, while fluxes of DON increase by 60%. This falling limb portion of discharge encompasses approximately 30% and 39% of Mackenzie River DIN and DON flux, suggesting that delta effects could subtract 4% from our DIN estimates and add 22% to our DON fluxes from this river. Although these modifications to our flux estimates are certainly notable, at our modeled tDON degradation rate of  $0.1 \text{ year}^{-1}$ , decreases in DIN flux to the ocean will largely be offset by increases in the availability of tDON-derived N. This, coupled with the fact that off-channel storage should be less important in smaller river deltas, indicates that delta effects should have a small impact on our overall estimates of the effect of riverine nutrients on oceanic primary productivity.

Over the Arctic Ocean as a whole, riverine nutrients do not support a large proportion of primary production. Our productivity estimates (as much as  $1.5 \text{ Tmol C year}^{-1}$ ) are just a fraction of the estimated  $11.3 \text{ Tmol C year}^{-1}$  of new production (Macdonald et al. 2010) or  $35 \text{ Tmol C year}^{-1}$  of total production (420 Tg; Pabi et al. 2008) that is generated throughout the Arctic basin. While riverine nutrients are available for uptake offshore in the form of tDON-derived inorganic N, their concentration is low in comparison to the total availability of DIN (e.g., Macdonald et al. 2010). It is in nearshore regions that riverine nutrients have the greatest influence on production: we estimate that nearshore primary production supported by terrigenous N may range as high as  $5.2 \text{ mol C m}^{-2} \text{ year}^{-1}$ , much of which comes from DIN. This is a large proportion of total nearshore production, which is estimated at  $8\text{--}12 \text{ mol C m}^{-2} \text{ year}^{-1}$  (Pabi et al. 2008). Further work, aimed explicitly at refining our estimates of the contribution of riverine nutrients to nearshore oceanic productivity, would greatly increase our understanding of biological processes in the Arctic Ocean.

In the future, several mechanisms could converge to increase the importance of riverine N in the Arctic Ocean nearshore. As the extent of Arctic sea ice continues to decline in all seasons (Serreze et al. 2007), the degree to which Arctic Ocean surface waters are exposed to UV radiation will increase. This, in turn, will be accompanied by increased rates of photoammonification of tDON, which should occur both earlier in the season and across a greater spatial extent. Using our estimated photoammonification rates, areas within the tDOM plume that remain ice-free from July through the end of September will regenerate  $\text{NH}_4$  at  $2.3 \text{ mmol NH}_4 \text{ m}^{-2}$ . This is nearly 10-fold the  $0.22 \text{ mmol m}^{-2}$  of photolytic  $\text{NH}_4$  release that we estimate to currently occur over this period, given present-day ice conditions and averaged over the extent of the tDOM



plume. In fact, photoammonification rates on tDOM from Arctic rivers may already be significantly higher than we calculate, given the lack of specific measurements available for Arctic river water and the wide known potential range for photoammonification AQYs. Additionally, the increased heating that will occur with decreased Arctic ice cover, coupled with increasing freshwater discharge from circumpolar rivers (Peterson et al. 2002; McClelland et al. 2006; Déry et al. 2009), could increase stratification in the Arctic nearshore, which could have the effect of trapping riverine nutrients closer to the ocean surface. Finally, it appears that nutrient loads in north-flowing rivers may also be trending upwards (Frey et al. 2007; McClelland et al. 2007). This work provides a first approximation of the current relative importance of tDON and tDIN to near- and offshore productivity in the Arctic Ocean and also assesses the relative importance of riverine N and DOC to oceanic food webs. Continued monitoring of the flux of riverine nutrients and organic matter from land to ocean should be an ongoing research priority, while work that specifically examines the importance of rivers to nearshore Arctic Ocean productivity should be highlighted as a pressing avenue for future research.

**Acknowledgments** Funding for this work was provided through NSF-OPP-0229302 and NSF-OPP-0732985. Support to SET was additionally provided by an NSERC Postdoctoral Fellowship. Greg Fiske assisted with GIS analysis. Comments by Rob Spencer and an anonymous reviewer significantly improved the content of this manuscript.

**Open Access** This article is distributed under the terms of the Creative Commons Attribution Noncommercial License which permits any noncommercial use, distribution, and reproduction in any medium, provided the original author(s) and source are credited.

## References

- Allen, A.E., M.H. Howard-Jones, M.G. Booth, M.E. Frischer, P.G. Verity, D.A. Bronk, and M.P. Sanderson. 2002. Importance of heterotrophic bacterial assimilation of ammonium and nitrate in the Barents Sea during summer. *Journal of Marine Systems* 38: 93–108.
- Alling, V., L. Sanchez-Garcia, D. Porcelli, S. Pugach, J.E. Vonk, B. van Dongen, C.-M. Mörth, L.G. Anderson, A. Sokolov, P. Andersson, C. Humborg, I. Semiletov, and Ö. Gustafsson. 2010. Nonconservative behavior of dissolved organic carbon across the Laptev and East Siberian seas. *Global Biogeochemical Cycles* 24: GB4033. doi:10.1029/2010GB003834.
- Amon, R.M.W., and R. Benner. 2003. Combined neutral sugars as indicators of the diagenetic state of dissolved organic matter in the Arctic Ocean. *Deep-Sea Research Part I—Oceanographic Research Papers* 50: 151–169.
- Bélangier, S., H.X. Xie, N. Krotkov, P. Larouche, W.F. Vincent, and M. Babin. 2006. Photomineralization of terrigenous dissolved organic matter in Arctic coastal waters from 1979 to 2003: Interannual variability and implications of climate change. *Global Biogeochemical Cycles* 20: GB4005. doi:10.1029/2006GB002708.
- Berglund, J., U. Muren, U. Bamstedt, and A. Andersson. 2007. Efficiency of a phytoplankton-based and a bacteria-based food web in a pelagic marine system. *Limnology and Oceanography* 52: 121–131.
- Booth, G., P. Raymond, and N.-H. Oh. 2007. *LoadRunner: Software and website*. Yale University: New Haven. <http://research.yale.edu/environment/loadrunner/>.
- Bronk, D.A., J.H. See, P. Bradley, and L. Killberg. 2007. DON as a source of bioavailable nitrogen for phytoplankton. *Biogeosciences* 4: 283–296.
- Brzezinski, M.A. 1985. The Si:C:N ratio of marine diatoms: Interspecific variability and the effect of some environmental variables. *Journal of Phycology* 21: 347–357.
- Bushaw, K.L., R.G. Zepp, M.A. Tarr, D. SchulzJander, R.A. Bourbonniere, R.E. Hodson, W.L. Miller, D.A. Bronk, and M. A. Moran. 1996. Photochemical release of biologically available nitrogen from aquatic dissolved organic matter. *Nature* 381: 404–407.
- Carlson, C.A. 2002. Production and removal processes. In *Biogeochemistry of marine dissolved organic matter*, ed. D.A. Hansell and C.A. Carlson, 91–151. San Diego: Academic.
- Carmack, E.C., R.W. Macdonald, and S. Jasper. 2004. Phytoplankton productivity on the Canadian Shelf of the Beaufort Sea. *Marine Ecology Progress Series* 277: 37–50.
- Condron, A., P. Winsor, C. Hill, and D. Menemenlis. 2009. Simulated response of the arctic freshwater budget to extreme NAO wind forcing. *Journal of Climate* 22: 2422–2437. doi:10.1175/2008jcli2626.1.
- Déry, S.J., and E.F. Wood. 2005. Decreasing river discharge in northern Canada. *Geophysical Research Letters* 32: L10401. doi:10.1029/2005gl022845.
- Déry, S.J., M.A. Hernandez-Henriquez, J.E. Burford, and E.F. Wood. 2009. Observational evidence of an intensifying hydrological cycle in northern Canada. *Geophysical Research Letters* 36: L13402. doi:10.1029/2009GL038852.
- Dittmar, T., H.P. Fitznar, and G. Kattner. 2001. Origin and biogeochemical cycling of organic nitrogen in the eastern Arctic Ocean as evident from D- and L-amino acids. *Geochimica Et Cosmochimica Acta* 65: 4103–4114.
- Dornblaser, M.M., and R.G. Striegl. 2007. Nutrient (N, P) loads and yields at multiple scales and subbasin types in the Yukon River basin, Alaska. *Journal of Geophysical Research-Biogeosciences* 112: G04S57. doi:10.1029/2006JG000366.
- Emmerton, C.A., L.F.W. Lesack, and W.F. Vincent. 2008. Mackenzie River nutrient delivery to the Arctic Ocean and effects of the Mackenzie Delta during open water conditions. *Global Biogeochemical Cycles* 22: GB1024. doi:10.1029/2006GB002856.
- Eppley, R.W., and B.J. Peterson. 1979. Particulate organic matter flux and planktonic new production in the deep ocean. *Nature* 282: 677–680.
- Fouilland, E., M. Gosselin, R.B. Rivkin, C. Vasseur, and B. Mostajir. 2007. Nitrogen uptake by heterotrophic bacteria and phytoplankton in Arctic surface waters. *Journal of Plankton Research* 29: 369–376.
- Frederick, J.E., and D. Lubin. 1988. The budget of biologically-active ultraviolet radiation in the earth-atmosphere system. *Journal of Geophysical Research—Atmospheres* 93: 3825–3832.
- Frey, K.E., and J.W. McClelland. 2009. Impacts of permafrost degradation on Arctic river biogeochemistry. *Hydrological Processes* 23: 169–182. doi:10.1002/hyp.7196.
- Frey, K.E., J.W. McClelland, R.M. Holmes, and L.C. Smith. 2007. Impacts of climate warming and permafrost thaw on the riverine transport of nitrogen and phosphorus to the Kara Sea. *Journal of Geophysical Research—Biogeosciences* 112: G04S58. doi:10.1029/2006JG000369.
- Garneau, M.E., M. Gosselin, B. Klein, J.E. Tremblay, and E. Fouilland. 2007. New and regenerated production during a late

- summer bloom in an Arctic polynya. *Marine Ecology Progress Series* 345: 13–26. doi:10.3354/meps06965.
- Goldman, J.C., D.A. Caron, O.K. Andersen, and M.R. Dennett. 1985. Nutrient cycling in a microflagellate food chain: I. Nitrogen dynamics. *Marine Ecology Progress Series* 24: 231–242.
- Goldman, J.C., D.A. Caron, and M.R. Dennett. 1987. Regulation of gross growth efficiency and ammonium regeneration in bacteria by substrate C:N ratio. *Limnology and Oceanography* 32: 1239–1252.
- Gordeev, V.V., J.M. Martin, I.S. Sidorov, and M.V. Sidorova. 1996. A reassessment of the Eurasian river input of water, sediment, major elements, and nutrients to the Arctic Ocean. *American Journal of Science* 296: 664–691.
- Gosselin, M., M. Levasseur, P.A. Wheeler, R.A. Horner, and B.C. Booth. 1997. New measurements of phytoplankton and ice algal production in the Arctic Ocean. *Deep Sea Research Part II: Topical Studies in Oceanography* 44: 1623–1644.
- Gueymard, C.A. 2001. Parameterized transmittance model for direct beam and circumsolar spectral irradiance. *Solar Energy* 71: 325–346.
- Gueymard, C.A. 2006. *SMARTS code, version 2.9.5 for Windows. User's manual.*
- Hansell, D.A., D. Kadko, and N.R. Bates. 2004. Degradation of terrigenous dissolved organic carbon in the western Arctic Ocean. *Science* 304: 858–861.
- Holmes, R.M., B.J. Peterson, V.V. Gordeev, A.V. Zhulidov, M. Meybeck, R.B. Lammers, and C.J. Vorosmarty. 2000. Flux of nutrients from Russian rivers to the Arctic Ocean: Can we establish a baseline against which to judge future changes? *Water Resources Research* 36: 2309–2320.
- Holmes, R.M., B.J. Peterson, A.V. Zhulidov, V.V. Gordeev, P.N. Makkaveev, P.A. Stunzhas, L.S. Kosmenko, G.H. Kohler, and A.I. Shiklomanov. 2001. Nutrient chemistry of the Ob' and Yenisey Rivers, Siberia: Results from June 2000 expedition and evaluation of long-term data sets. *Marine Chemistry* 75: 219–227.
- Holmes, R.M., J.W. McClelland, B.J. Peterson, I.A. Shiklomanov, A.I. Shiklomanov, A.V. Zhulidov, V.V. Gordeev, and N.N. Bobrovitskaya. 2002. A circumpolar perspective on fluvial sediment flux to the Arctic Ocean. *Global Biogeochemical Cycles* 16: 1098. doi:10.1029/2001GB001849.
- Holmes, R.M., J.W. McClelland, B.J. Peterson, S.E. Tank, E. Buluygina, T.I. Eglinton, V.V. Gordeev, T.Y. Gurtovaya, P.A. Raymond, D.J. Repeta, R. Staples, R.G. Striegl, A.V. Zhulidov, and S.A. Zimov. 2011. Seasonal and annual fluxes of nutrients and organic matter from large rivers to the Arctic Ocean and surrounding seas. *Estuaries and Coasts*. doi:10.1007/s12237-011-9386-6.
- Hopkinson, C.S., and J.J. Vallino. 2005. Efficient export of carbon to the deep ocean through dissolved organic matter. *Nature* 433: 142–145. doi:10.1038/nature03191.
- Hopkinson, C.S., I. Buffam, J. Hobbie, J. Vallino, M. Perdue, B. Eversmeyer, F. Prahl, J. Covert, R. Hodson, M.A. Moran, E. Smith, J. Baross, B. Crump, S. Findlay, and K. Foreman. 1998. Terrestrial inputs of organic matter to coastal ecosystems: An intercomparison of chemical characteristics and bioavailability. *Biogeochemistry* 43: 211–234.
- Jakobsson, M. 2002. Hypsometry and volume of the Arctic Ocean and its constituent seas. *Geochemistry Geophysics Geosystems* 3: 1028. doi:10.1029/2001GC000302.
- Joint, I., P. Henriksen, G.A. Fonnes, D. Bourne, T.F. Thingstad, and B. Riemann. 2002. Competition for inorganic nutrients between phytoplankton and bacterioplankton in nutrient manipulated mesocosms. *Aquatic Microbial Ecology* 29: 145–159.
- Kattner, G., J.M. Lobbes, H.P. Fitznar, R. Engbrodt, E.M. Nothig, and R.J. Lara. 1999. Tracing dissolved organic substances and nutrients from the Lena River through Laptev Sea (Arctic). *Marine Chemistry* 65: 25–39.
- Kirchman, D.L. 1994. The uptake of inorganic nutrients by heterotrophic bacteria. *Microbial Ecology* 28: 255–271.
- Kirchman, D.L., V. Hill, M.T. Cottrell, R. Gradinger, R.R. Malmstrom, and A. Parker. 2009. Standing stocks, production, and respiration of phytoplankton and heterotrophic bacteria in the western Arctic Ocean. *Deep-Sea Research Part II—Topical Studies in Oceanography* 56: 1237–1248. doi:10.1016/j.dsr2.2008.10.018.
- Lammers, R.B., A.I. Shiklomanov, C.J. Vorosmarty, B.M. Fekete, and B.J. Peterson. 2001. Assessment of contemporary Arctic river runoff based on observational discharge records. *Journal of Geophysical Research—Atmospheres* 106: 3321–3334.
- Letscher, R.T., D.A. Hansell, and D. Kadko. 2011. Rapid removal of terrigenous dissolved organic carbon over the Eurasian shelves of the Arctic Ocean. *Marine Chemistry* 123: 78–87. doi:10.1016/j.marchem.2010.10.002.
- Macdonald, R.W., E. Sakshaug, and R. Stein. 2004. The Arctic Ocean: Modern status and recent climate change. In *The organic carbon cycle in the Arctic Ocean*, ed. R. Stein and R.W. Macdonald, 6–21. Berlin: Springer.
- Macdonald, R.W., L.G. Anderson, J.P. Christensen, L.A. Miller, I.P. Semiletov, and R. Stein. 2010. The Arctic Ocean. In *Carbon and nutrient fluxes in continental margins: A global synthesis*, ed. K.-K. Liu, L. Atkinson, R. Quinones, and L. Talae-McManus. Berlin: Springer.
- Manizza, M., M.J. Follows, S. Dutkiewicz, J.W. McClelland, D. Menemenlis, C.N. Hill, A. Townsend-Small, and B.J. Peterson. 2009. Modeling transport and fate of riverine dissolved organic carbon in the Arctic Ocean. *Global Biogeochemical Cycles* 23: GB4006. doi:10.1029/2008GB003396.
- Manizza, M., M.J. Follows, S. Dutkiewicz, D. Menemenlis, J.W. McClelland, C.N. Hill, B.J. Peterson, and R. Key. 2011. A model of the arctic ocean carbon cycle. *Journal of Geophysical Research—Oceans* (in review).
- Marshall, J., C. Hill, L. Perelman, and A. Adcroft. 1997. Hydrostatic, quasi-hydrostatic, and nonhydrostatic ocean modeling. *Journal of Geophysical Research—Oceans* 102: 5733–5752. doi:10.1029/96JC02776.
- McClelland, J.W., S.J. Dery, B.J. Peterson, R.M. Holmes, and E.F. Wood. 2006. A Pan-Arctic evaluation of changes in river discharge during the latter half of the 20th century. *Geophysical Research Letters* 33: L06715. doi:10.1029/2006GL025753.
- McClelland, J.W., M. Stieglitz, F. Pan, R.M. Holmes, and B.J. Peterson. 2007. Recent changes in nitrate and dissolved organic carbon export from the upper Kuparuk River, North Slope, Alaska. *Journal of Geophysical Research—Biogeosciences* 112: G04S60. doi:10.1029/2006JG000371.
- McClelland, J.W., R.M. Holmes, B.J. Peterson, R. Amon, T. Brabets, L. Cooper, J. Gibson, V.V. Gordeev, C. Guay, D. Milburn, R. Staples, P.A. Raymond, I. Shiklomanov, R. Striegl, A. Zhulidov, T. Gurtovaya, and S. Zimov. 2008. Development of a Pan-Arctic database for river chemistry. *Eos Trans. AGU* 89: 217–218. doi:10.1029/2008EO240001.
- McClelland, J.W., A. Townsend-Small, R.M. Holmes, F. Pan, M. Stieglitz, M. Khosh, and B.J. Peterson. 2011a. Nutrient and organic matter export from the North Slope of Alaska to the Beaufort Sea. *Journal of Geophysical Research—Biogeosciences* (in review).
- McClelland, J.W., R.M. Holmes, K.H. Dunton, and R.W. Macdonald. 2011b. The Arctic Ocean estuary. *Estuaries and Coasts*. doi:10.1007/s12237-010-9357-3.
- McLaughlin, F., K. Shimada, E. Carmack, M. Itoh, and S. Nishino. 2005. The hydrography of the southern Canada Basin, 2002. *Polar Biology* 28: 182–189. doi:10.1007/s00300-004-0701-6.

- Menemenlis, D., C. Hill, A. Adcroft, J.-M. Campin, B. Cheng, B. Ciotti, I. Fukumori, P. Heimbach, C. Henze, A. Köhl, T. Lee, D. Stammer, J. Taft, and J. Zhang. 2005. NASA supercomputer improves prospects for ocean climate research. *Eos Trans. AGU* 86: 89.
- Meon, B., and R.M.W. Amon. 2004. Heterotrophic bacterial activity and fluxes of dissolved free amino acids and glucose in the Arctic rivers Ob, Yenisei and the adjacent Kara Sea. *Aquatic Microbial Ecology* 37: 121–135.
- Mulholland, M.R., P.M. Glibert, G.M. Berg, L. Van Heukelem, S. Pantoja, and C. Lee. 1998. Extracellular amino acid oxidation by microplankton: A cross-ecosystem comparison. *Aquatic Microbial Ecology* 15: 141–152.
- Opsahl, S., R. Benner, and R.M.W. Amon. 1999. Major flux of terrigenous dissolved organic matter through the Arctic Ocean. *Limnology and Oceanography* 44: 2017–2023.
- Pabi, S., G.L. van Dijken, and K.R. Arrigo. 2008. Primary production in the Arctic Ocean, 1998–2006. *Journal of Geophysical Research—Oceans* 113: C08005. doi:10.1029/2007JC004578.
- Peterson, B.J., R.M. Holmes, J.W. McClelland, C.J. Vorosmarty, R.B. Lammers, A.I. Shiklomanov, I.A. Shiklomanov, and S. Rahmstorf. 2002. Increasing river discharge to the Arctic Ocean. *Science* 298: 2171–2173.
- Raymond, P.A., J.W. McClelland, R.M. Holmes, A.V. Zhulidov, K. Mull, B.J. Peterson, R.G. Striegl, G.R. Aiken, and T.Y. Gurtovaya. 2007. Flux and age of dissolved organic carbon exported to the Arctic Ocean: A carbon isotopic study of the five largest arctic rivers. *Global Biogeochemical Cycles* 21: GB4011. doi:10.1029/2007GB002934.
- Runkel, R.L., C.G. Crawford, and T.A. Cohn. 2004. LoadEstimator (LOADEST): A FORTRAN Program for estimating constituent loads in streams and rivers. In *U.S. Geological Survey Techniques and Methods Book 4, Chapter A5*, 69 pp.
- Serreze, M.C., M.M. Holland, and J. Stroeve. 2007. Perspectives on the Arctic's shrinking sea-ice cover. *Science* 315: 1533–1536. doi:10.1126/science.1139426.
- Simpson, K.G., J.E. Tremblay, Y. Gratton, and N.M. Price. 2008. An annual study of inorganic and organic nitrogen and phosphorus and silicic acid in the southeastern Beaufort Sea. *Journal of Geophysical Research—Oceans* 113: C07016. doi:10.1029/2007JC004462.
- Smith, W., M. Gosselin, L. Legendre, D. Wallace, K. Daly, and G. Kattner. 1997. New production in the Northeast Water Polynya: 1993. *Journal of Marine Systems* 10: 199–209.
- Stedmon, C.A., and S. Markager. 2001. The optics of chromophoric dissolved organic matter (CDOM) in the Greenland Sea: An algorithm for differentiation between marine and terrestrially derived organic matter. *Limnology and Oceanography* 46: 2087–2093.
- Stedmon, C.A., S. Markager, L. Tranvik, L. Kronberg, T. Slatis, and W. Martinsen. 2007. Photochemical production of ammonium and transformation of dissolved organic matter in the Baltic Sea. *Marine Chemistry* 104: 227–240. doi:10.1016/j.marchem.2006.11.005.
- Stedmon, C.A., R.M.W. Amon, A.J. Rinehart, and S.A. Walker. 2011. The supply and characteristics of colored dissolved organic matter (CDOM) in the Arctic Ocean: Pan Arctic trends and differences. *Marine Chemistry* 124: 108–118.
- Stone, R.S., G.P. Anderson, E.P. Shettle, E. Andrews, K. Loukachine, E.G. Dutton, C. Schaaf, and M.O. Roman. 2008. Radiative impact of boreal smoke in the Arctic: Observed and modeled. *Journal of Geophysical Research—Atmospheres* 113: D14S16. doi:10.1029/2007JD009657.
- Striegl, R.G., G.R. Aiken, M.M. Dornblaser, P.A. Raymond, and K.P. Wickland. 2005. A decrease in discharge-normalized DOC export by the Yukon River during summer through autumn. *Geophysical Research Letters* 32: L21413. doi:10.1029/2005GL024413.
- Sun, L., E.M. Perdue, J.L. Meyer, and J. Weis. 1997. Use of elemental composition to predict bioavailability of dissolved organic matter in a Georgia river. *Limnology and Oceanography* 42: 714–721.
- Tank, S.E. 2009. *Sources and cycling of dissolved organic carbon across a landscape of Arctic delta lakes*. Burnaby, BC, Canada: Simon Fraser University.
- Tremblay, J.É., and J. Gagnon. 2009. The effects of irradiance and nutrient supply on the productivity of Arctic waters: A perspective on climate change. In *Influence of climate change on the changing Arctic and Sub-Arctic*, ed. J.C.J. Nihoul and A. G. Kostianoy, 73–93. New York: Springer.
- Tremblay, J.É., C. Michel, K.A. Hobson, M. Gosselin, and N.M. Price. 2006. Bloom dynamics in early opening waters of the Arctic Ocean. *Limnology and Oceanography* 51: 900–912.
- Vähätalo, A.V., and R.G. Zepp. 2005. Photochemical mineralization of dissolved organic nitrogen to ammonium in the Baltic Sea. *Environmental Science & Technology* 39: 6985–6992. doi:10.1021/es050142z.
- Walker, H.J. 1998. Arctic deltas. *Journal of Coastal Research* 14: 718–738.
- Walsh, J.J., D.A. Dieterle, W. Maslowski, J.M. Grebmeier, T.E. Whittedge, M. Flint, I.N. Sukhanova, N. Bates, G.F. Cota, D. Stockwell, S.B. Moran, D.A. Hansell, and C.P. McRoy. 2005. A numerical model of seasonal primary production within the Chukchi/Beaufort Seas. *Deep-Sea Research Part II—Topical Studies in Oceanography* 52: 3541–3576. doi:10.1016/j.dsr2.2005.09.009.
- Walvoord, M.A., and R.G. Striegl. 2007. Increased groundwater to stream discharge from permafrost thawing in the Yukon River basin: Potential impacts on lateral export of carbon and nitrogen. *Geophysical Research Letters* 34: L12402. doi:10.1029/2007GL030216.